Free Radical Biology and Medicine 227 (2025) 246–259

Contents lists available at ScienceDirect

Free Radical Biology and Medicine

journal homepage: www.elsevier.com/locate/freeradbiomed

NADPH oxidase 4-SH3 domain-containing YSC84-like 1 complex participates liver inflammation and fibrosis

Yeo Kyu Hur [a,1], Hye Eun Lee [b,1], Jung-Yeon Yoo [a], Young Nyun Park [c], In Hye Lee [a,**], Yun Soo Bae [a,b,*]

[a] Department of Life Sciences, Ewha Womans University, 52 Ewhayeodae-Gil, Seodaemoon-Gu, Seoul, 03760, South Korea
[b] Celros Biotech, 52 Ewhayeodae-Gil, Seodaemoon-Gu, Seoul, 03760, South Korea
[c] Department of Pathology Yonsei University College of Medicine, 50 Yonsei-ro, Seodaemun-Gu, Seoul, 03722, South Korea

ARTICLE INFO

Keywords:
Nox4
SH3YL1
Reactive oxygen species
Metabolic dysfunction-associated steatohepatitis
Fibrosis

ABSTRACT

There is growing evidence that NADPH oxidase 4 (Nox4) in hepatocytes contributes to liver inflammation and fibrosis during the development of metabolic dysfunction-associated steatohepatitis (MASH). However, how Nox4 is regulated and leads to liver pathogenesis is unclear. Our previous studies showed that the cytosolic protein SH3 domain-containing Ysc84-like 1 (SH3YL1) regulates Nox4 activity. Here, we asked whether SH3YL1 also participates in liver inflammation and fibrosis during MASH development. We generated that whole body SH3YL1 knockout (SH3YL1$^{-/-}$), Nox4 knockout (Nox4$^{-/-}$) mice, and the hepatocyte-specific SH3YL1 conditional knockout (Alb-Cre/SH3YL1$^{fl/fl}$) mice were fed a methionine/choline-deficient (MCD) diet to induce liver inflammation and fibrosis in pathogenesis of MASH. Palmitate-stimulated primary SH3YL1-and Nox4-deficient hepatocytes and hepatic stellate cells (HSCs) did not generate H_2O_2. While the liver of MCD diet-fed wild type (WT) mice demonstrated elevated 3-nitrotyrosine as a protein oxidation and 4-hydroxynonenal adducts as a lipid oxidation and increased liver inflammation, hepatocyte apoptosis, and liver fibrosis, these events were markedly reduced in SH3YL1$^{-/-}$, Nox4$^{-/-}$, and Alb-Cre/SH3YL1$^{fl/fl}$ mice. The MCD diet-fed WT mice also showed elevated hepatocyte expression of SH3YL1 protein. Similarly, liver biopsies from MASH patients demonstrated strong hepatocyte SH3YL1 protein expression, whereas hepatocytes from patients with steatosis weakly expressed SH3YL1 and histologically normal patient hepatocytes exhibited very little SH3YL1 expression. The Nox4-SH3YL1 complex in murine hepatocytes elevates their H_2O_2 production, which promotes the liver inflammation, hepatocyte apoptosis, and liver fibrosis that characterize MASH. This axis may also participate in MASH in humans.

1. Background

Metabolic dysfunction-associated fatty-liver disease (MAFLD) (previously known as nonalcoholic fatty-liver disease) is a broad spectrum of chronic liver diseases that are characterized by accumulation of fat in the liver [1–3]. They include metabolic dysfunction-associated fatty liver (MAFL), which does not involve liver injury or inflammation, and metabolic dysfunction-associated steatohepatitis (MASH), which is an advanced stage of steatosis that is characterized by hepatocellular ballooning and injury, inflammation, and fibrosis. MASH is a key risk factor for cirrhosis and hepatocellular carcinoma [2,4]. MAFLD is the most common cause of chronic liver disease worldwide: 10–40 % and 2–5% of the adults in the United States of America are respectively estimated to have a form of MAFLD and specifically MASH [5,6]. The mechanisms that underlie the development and progression of MASH are incompletely understood but proposed risk factors include: insulin

Abbreviations: 3-NT, 3-Nitrotyrosine; 4-HNE, 4-Hydroxynonenal; ECM, Extracellular matrix; MAFLD, Metabolic dysfunction-associated fatty liver disease; MASH, Metabolic dysfunction-associated steatohepatitis; MCD, Methionine/choline–deficient diet; MCS, Methionine/choline-sufficient diet; Nox, NADPH-Oxidase; ROS, Reactive-oxygen species; RT, Room temperature; SH3YL1, Src homology 3 (SH3) domain-containing Ysc84-like 1.

* Corresponding author. Department of Life Sciences, Ewha Womans University, Seoul, South Korea.
** Corresponding author. Department of Life Sciences, Ewha Womans University, Seoul, South Korea.
E-mail addresses: lih3026@ewha.ac.kr (I.H. Lee), baeys@ewha.ac.kr (Y.S. Bae).
[1] These authors contributed equally to this work.

https://doi.org/10.1016/j.freeradbiomed.2024.12.021
Received 31 August 2024; Received in revised form 19 November 2024; Accepted 4 December 2024
Available online 5 December 2024

resistance and the accumulation of fat in the liver which is toxic and induces mitochondrial dysfunction [7]; production of reactive oxygen species (ROS) [8]; endoplasmic reticulum (ER) stress [8]; altered gut flora which amplifies the production of fatty acids in the bowel [9], and genetic factors or epigenetic modification [10]. In particular, oxidative stress and ROS production are closely linked to hepatic inflammation and fibrosis in MASH pathogenesis [8,11,12].

While low ROS levels are needed for normal cellular functions such as proliferation and differentiation [13–16], abnormally high ROS levels are cytotoxic because they generate lipid and protein oxidation products (e.g. 4-HNE and 3-NT). MASH is characterized by high ROS levels and oxidative stress in hepatocytes, and considerable evidence indicates that this promotes the hallmark liver inflammation, hepatocyte death, and fibrosis of this disease [17–20]. Important generators of these hepatic ROS include the mitochondrial respiratory chain, cyclooxygenase, fatty-acid metabolism, and the NADPH oxidase (Nox) isozymes. Recently, Nox was found to be a major source of ROS production in pathogenesis of MASH. Seven human Nox isozymes (Nox1, Nox2, Nox3, Nox4, Nox5, Duox1 and Duox2) have been identified in human [15]. The main ROS-producing Nox isozymes in the liver are Nox1, Nox2, and Nox4 [12]. Hepatocytes mainly express Nox4, and this expression is elevated in MASH patients and animal models of MASH. Moreover, hepatocyte-specific knockout of Nox4 in mouse models of MASH (i.e. mice fed a choline-deficient L-amino acid-defined diet or a high-fat and high-fructose diet) attenuates their ROS levels, lipid peroxidation, inflammation, and fibrosis in the liver [21]. Similarly, when mice with whole body knockout of Nox1 or Nox4 are treated with carbon tetrachloride (CCl_4) to induce liver fibrosis, they demonstrate less liver inflammation, injury, and fibrosis than wild type (WT) mice [22]. Thus, hepatocyte Nox expression may promote MASH.

Since excessive ROS levels are highly toxic, the activation of Nox isozymes is tightly regulated. For example, Nox1-3 are well known to be regulated by their interactions with cytosolic activator (Noxa1 for Nox1/3 and $p67^{phox}$ for Nox2) and organizer (Noxo1 for Nox1/3 and $p47^{phox}$ for Nox2) subunits. Moreover, the membrane protein p22phox binds to Nox1-4 and is essential for the ROS-producing capacity of these isozymes [15]. However, how Nox4, the main hepatocyte isozyme, is regulated remains incompletely understood. Our previous studies may shed some light: we reported that when renal tubular-epithelial cells are subjected to oxidative stress induced by lipopolysaccharide (LPS) or transforming-growth factor-β1 (TGFβ1), a cytosolic protein called SH3 domain-containing Ysc84-like 1 (SH3YL1) participates in Nox4 activation. Specifically, it constitutively binds to the COOH-terminal region of Nox4 and its LPS/TGFβ1-mediated phosphorylation induces its SH3 domain to transiently interact with the proline-rich region (PRR) of $p22^{phox}$. This triggers the formation of a ternary $p22^{phox}$-SH3YL1-Nox4 complex. Our studies then showed with whole body and conditional podocyte-specific knockout of SH3YL1 that the ternary $p22^{phox}$--SH3YL1-Nox4 complex drives LPS-induced acute-kidney injury and TGFβ1-induced diabetic nephropathy [23,24].

These observations led us to examine the role of SH3YL1 in liver inflammation and fibrosis during MASH in the present study. We found that SH3YL1 stimulates Nox4 activity in hepatocytes and that this leads to hepatic oxidative stress in the liver. This in turn induces inflammation, hepatocyte injury, and fibrosis in the liver that contribute to MASH pathogenesis. Thus, the SH3YL1-Nox4 complex helps drive liver inflammation and fibrosis during MASH, which suggests that it could be a potential therapeutic target for MASH.

2. Materials and methods

2.1. Antibodies

Rabbit polyclonal antibody to Nox4 was produces using a mixture of synthetic peptides (DGIQKIIGEKY, RPRWKLLFDEIAK and RFEYNKESFS) as described previously.[23] Anti-SH3YL1 antibody was purchased (#NBP1-84133; Novus; Centennial CO, USA). The following antibodies were also purchased: anti-Nox1 (#ab131088; Abcam); anti-Nox2 (#ab80897; Abcam); anti-$p22^{phox}$ (#ab75941; Abcam); anti-α-tubulin antibody (#LF-MA0117; Abfrontier); anti-Flag antibody (#F3165; Sigma Aldrich); anti-collagen I (#ab34710) and F4/80 (#ab6640) (both from Abcam; Cambridge, MA, USA); anti-E-cadherin antibody (#610182; BD Biosciences; San Jose, CA, USA); anti-3-nitrotyrosine (3-NT) antibody (#AB5411; Millipore; Carlsbad, CA, USA); and anti-4-hydroxynonenal (4-HNE) antibody (#MHN-020P; JaICA; Fukuroi, Shizuoka, Japan).

2.2. Generation of hepatocyte-specific SH3YL1 KO mice

Albumin-specific SH3YL1 knockout Alb-Cre/$SH3YL1^{fl/fl}$ mice were generated from $SH3YL1^{flox/+}$ mice after exposure to flp recombinase. Heterozygous SH3YL1 floxed mice were crossed with B6.Cg-Tg(Alb-cre) 21Mgn/J mice that were obtained from Ewha Womans University. To acquire homozygous floxed-SH3YL1 mice with Alb-Cre transgene, Alb-Cre/$SH3YL^{flox/+}$ mice were crossed with $SH3YL1^{flox/+}$ without Alb-Cre transgene. (Alb-Cre/SH3YL1fl/fl): these mice thus lacked SH3YL1 in hepatocytes only. To genotype mice, DNA was isolated from the tails and subjected to RT-PCR method using MyTaq HS DNA Polymerase (Bioline, #BIO-21111, Humber Road, London, UK), and the following primers: CGC0052 5′-ACC TGA AGA TGT TCG CGA TTA TCT-3’; CGC0053 5′-ACC GTC AGT ACG TGA GAT ATC TT-3’; CSD-loxF 5′ GAG ATG GCG CAA CGC AAT TAA TG 3’; CSD-SH3YL1-R 5′ TCA CAT GGA GGT GCT ATA GAA GGG C 3’; and CSD- SH3YL1-F 5′ TGA GGT ATG TTC TGT GCT GAG ACC C 3’; CSD- SH3YL1-ttR 5′ CTT TGC GTA GAT AAG GCC AGA AGC C 3’. The following primer sets were used: (1) Alb-Cre primer set: CGC0052/CGC0053; (2) Wild-type/PostFlp primer set: CSD-SH3YL1-F/CSD-SH3YL1-ttR; and (3) Floxed primer set: CSD-loxF/CSD-SH3YL1-R.

2.3. Mice and the methionine choline deficient diet-induced MASH model

All mice used in this study were on the C57BL/6 background. Conventional whole-body $SH3YL1^{-/-}$ and $Nox4^{-/-}$ knockout mice were generated as described previously [23]. We also generated hepatocyte-specific SH3YL1-knockout (Alb-Cre/$SH3YL1^{fl/fl}$) mice (see next section). 8-week-old WT, $SH3YL1^{-/-}$, $Nox4^{-/-}$, and Alb-Cre/-$SH3YL1^{fl/fl}$ mice were fed a methionine/choline-deficient diet (MCD) (A02082002BR; Research Diet, New Brunswick, NJ) or, as a control, a methionine/choline-sufficient diet (MCS) (A02082003BY; Research Diet, New Brunswick, NJ) for 8 weeks. All animals were housed in a room under controlled temperature and humidity conditions and in a 12h-light/12h-dark cycle. The study protocol was approved by the Animal Subjects Committee of Ewha Womans University (Seoul, Korea). All animal-related procedures were approved by the Institutional Animal Care and Use Committee (IACUC) and were conducted with ethical guidance by Ewha Womans University.

2.4. Human samples

Paraffin-embedded liver samples from patients with histologically determined healthy liver (n = 7), steatosis (n = 5), or MASH (n = 7) were obtained from Yonsei University, School of Medicine (Seoul, Korea). This study was approved by the Human Research Protection Center (IRB 4-2018-1118) of the Yonsei University Health System. Written consent was given in writing by all subjects.

2.5. Statistical analyses

The quantitative data were expressed as the mean ± SEM and analyzed with *t*-test, one-way ANOVA, or mixed effect analysis.

3. Results

3.1. SH3YL1 interacts with Nox4-p22phox complex and stimulates Nox4-dependent H_2O_2 production in primary hepatocytes

Our previous studies showed that when renal tubular-epithelial cells are stimulated with LPS or TGFβ, the ternary SH3YL1-Nox4-$p22^{phox}$ complex is generated and Nox4 is activated and produces H_2O_2 [23,24]. Since the saturated fatty acid palmitate (i) induces hepatocyte apoptosis, (ii) is more hepatotoxic than other saturated and unsaturated fatty acids, and (iii) is strongly linked to MASLD/MASH [25–27], we speculated that palmitate stimulation could induce the formation of the SH3YL1--Nox4-$p22^{phox}$ complex in primary hepatocytes and hepatic stellate LX-2 cells. To test this, primary WT murine hepatocytes and LX-2 cells were treated with or without palmitate, their lysates were immunoprecipitated with an anti-SH3YL1 antibody, and the presence of Nox4 or $p22^{phox}$ in the immunoprecipitates was probed with specific antibodies. Palmitate did not alter the constitutive interaction between SH3YL1 and Nox4. However, it did induce SH3YL1 to interact with $p22^{phox}$. Thus, palmitate indeed generated the ternary SH3YL1-Nox4-$p22^{phox}$ complex in hepatocytes and LX-2 cells (Fig. 1A and B). We also showed that this complex formation associated with H_2O_2 production by the primary hepatocytes and hepatic stellate cells (HSCs), as shown with Peroxy Orange-1, a fluorescent probe for imaging H_2O_2. By contrast, primary hepatocytes and hepatic stellate cells (HSCs) from whole-body $SH3YL1^{-/-}$ and $Nox4^{-/-}$ mice did not produce H_2O_2 in response to palmitate (Fig. 1C, D, and S1). Moreover, expression levels of Nox1, Nox2, Nox4 and p22phox in liver tissues of $SH3YL1^{-/-}$ mice were similar with that in WT (Fig. S2).

To confirm the link between Nox4 and SH3YL1 in palmitate-induced H_2O_2 generation, SH3YL1 was overexpressed in $SH3YL1^{-/-}$ hepatocytes. Indeed, this induced not only SH3YL1 levels in $SH3YL1^{-/-}$ hepatocytes to recover, it also restored their palmitate-induced H_2O_2 production (Fig. 1E and F). Thus, SH3YL1 plays an essential role in palmitate-stimulated Nox4-$p22^{phox}$-dependent H_2O_2 production by hepatocytes.

3.2. Hepatocyte expression of SH3YL1 is elevated in mice with MCD-induced MASH and in MASH patients

We hypothesized whether SH3YL1 expression is elevated during the pathogenesis of MASH animal model. Indeed, palmitate-stimulated primary WT hepatocytes exhibited increased SH3YL1 expression (Fig. 2A). Moreover, MCD diet-fed WT mice demonstrated significantly elevated SH3YL1 expression in their liver and hepatocytes, as shown by immunoblot and immunohistochemistry (Fig. 2B and C). Next, we investigated SH3YL1 expression in liver tissue from histologically normal feature, and steatosis and MASH patients. The liver biopsy procedure was approved by the Research and Education Institute Investigational Review Board at Yonsei University Medical Center and informed consent was obtained from each patient. All liver biopsy patients were enrolled at the Yonsei University Medical Center. Notably, we also observed significantly higher SH3YL1 expression in liver biopsies from MASH patients. Specifically, histologically normal liver biopsies from control patients showed very little SH3YL1 expression in the hepatocytes while the liver biopsies from steatosis patients demonstrated slightly increased SH3YL1 expression. By contrast, the hepatocytes of MASH patients showed very high SH3YL1 expression (arrows in Fig. 2D). Thus, hepatocyte activation may be linked to SH3YL1 expression in MASH patients, which suggests that SH3YL1 expression associates with the progression of the steatotic liver to MASH.

3.3. MCD diet-fed $SH3YL1^{-/-}$ and $Nox4^{-/-}$ mice demonstrate suppressed hepatic ROS levels and hepatic lipid accumulation

To evaluate the role of SH3YL1-Nox4 in MASH, whole-body $SH3YL1^{-/-}$ and $Nox4^{-/-}$ mice were fed a MCD diet, which induces MASH (Fig. 3A). As a control, the mice were fed a MCS diet (Fig. 3A). Since oxidative stress is a hallmark feature of MASH progression [28], the liver were assessed for 3-nitrotyrosine (3-NT) (a protein oxidation marker), 4-hydroxynonenal (4-HNE) adducts (a lipid oxidation marker), and malonaldehyde (lipid peroxidation marker). Immunohistochemistry with anti-3-NT and anti-4-HNE antibodies showed that both markers were strongly elevated in the liver of MCD diet-fed WT but attenuated in MCD diet-fed $SH3YL1^{-/-}$ and $Nox4^{-/-}$ mouse livers (Fig. 3B–D). This pattern was also observed when malondialdehyde in liver extracts was measured by examining the TBARS levels (Fig. 3E). Additionally, we found that the co-localization of SH3YL1 with p22phox was increased in liver tissue of MCD diet-fed WT, compared to that of MCS diet-fed WT (arrow heads in Fig. S3). Thus, SH3YL1-Nox4-dependent H_2O_2 generation associates with oxidative stress in MASH.

It is well known that MASH is characterized by fat accumulation in the liver [29]. Indeed, H&E-staining of the liver from MCD diet-fed WT mice revealed increased lipid-droplet numbers compared to MCS diet-fed WT mice. However, the MCD diet-induced number and size of lipid-droplets were not affected by SH3YL1 or Nox4 deficiency (Fig. 3F and S4). However, analysis of triglycerides (TG) in liver tissue revealed a 30 % reduction in SH3YL1 KO and Nox4 KO mice compared to WT (Fig. S5A). Additionally, liver tissues from $SH3YL1^{-/-}$ and $Nox4^{-/-}$ mice exhibited reduced oil red O staining compared to WT (Fig. S5B). These results suggest that SH3YL1 is involved in fat accumulation in response to the MCD diet.

3.4. MCD diet-fed $SH3YL1^{-/-}$ and $Nox4^{-/-}$ mice exhibit suppressed liver inflammation, hepatocyte injury, and liver fibrosis

Hepatic inflammation is an important factor in MASH onset [30,31]. Indeed, the liver of MCD diet-fed WT mice demonstrated elevated mRNA levels of the pro-inflammatory cytokines TNF-α, IL-1β, IL-6, TIMP-1, Cxcl-2, Ccl-3, Ccl-4, and MCP-1 in the liver. However, this was strongly suppressed by SH3YL1 or Nox4 deficiency (Fig. 4). Interestingly, although the liver of MCD diet-fed WT mice exhibited elevated levels of F4/80 in histological analysis (Fig. 5A, left panel of Fig. 5B) and mRNA level of F4/80 (right panel of Fig. 5B), which is a marker of macrophage infiltration, this elevation was significantly more muted in the liver from MCD diet-fed $SH3YL1^{-/-}$ and $Nox4^{-/-}$ mice (Fig. 5A and B). Thus, SH3YL1 and Nox4 contribute to hepatic inflammation in MASH.

It is well-established that fat accumulation in the liver injures the liver, at least in part because free fatty acids induce pro-apoptotic signaling and multiple stress responses in hepatocytes [32–34]. Indeed, MCD diet-fed WT mice developed marked hepatocyte apoptosis, as shown by TUNEL staining of the liver. However, this hepatocyte apoptosis was significantly suppressed in MCD diet-fed $SH3YL1^{-/-}$ and $Nox4^{-/-}$ mice (Fig. 5C and D). The role of the SH3YL1-Nox4 axis in hepatocyte apoptosis was further tested in vitro. Indeed, palmitate-treated primary hepatocytes from WT mice demonstrated apoptosis, but this was suppressed in primary hepatocytes from $SH3YL1^{-/-}$ and $Nox4^{-/-}$ mice (Fig. S6). Thus, the SH3YL1-Nox4 axis may cause the hepatic injury that leads to MASH.

Hepatic inflammation and injury are the major causes of hepatic fibrosis [35]. We found that while MCD diet-fed WT mice demonstrated hepatic fibrosis, as determined by Masson's trichrome staining for collagen expression, IHC analysis of α-SMA expression (Fig. 6A–C), and Sirius red staining (Fig. S7), this was significantly attenuated in MCD diet-fed $SH3YL1^{-/-}$ and $Nox4^{-/-}$ mice. Moreover, while liver extracts from MCD diet-fed WT mice demonstrated elevated the protein and mRNA levels of collagen type I and α-SMA, this was significantly reduced in SH3YL1-and Nox4-deficient mice (Fig. 6D and E). In addition, the MCD diet-fed WT mice showed elevated mRNA expression of the fibrosis markers TGFβ1, vimentin, and fibronectin in their liver but this was suppressed in SH3YL1-and Nox4-deficient mice (Fig. 6F). Thus, the SH3YL1-Nox4 complex may contribute to the liver fibrosis in MASH.

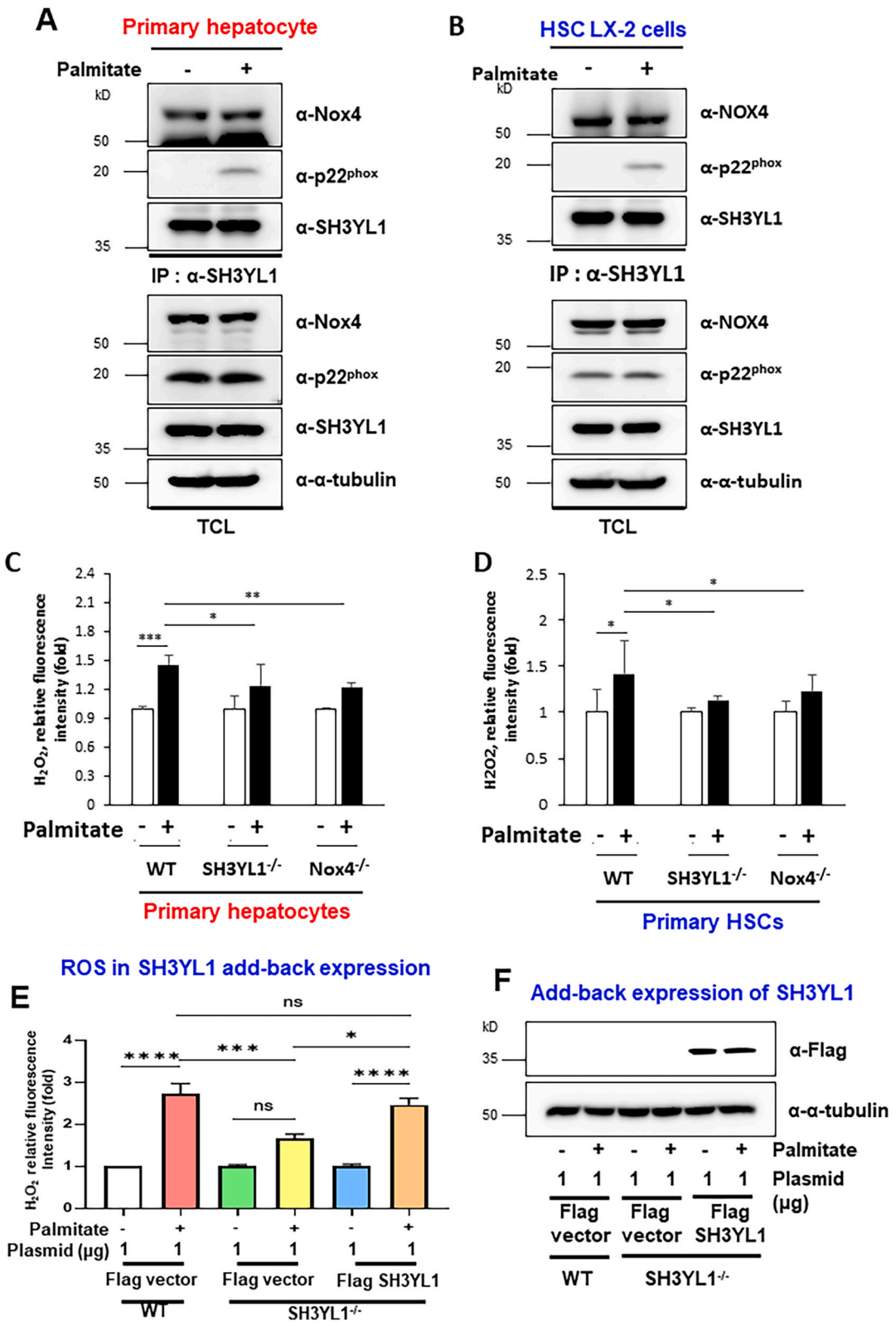

Fig. 1. Effect of SH3YL1 or Nox4 deficiency on palmitate-induced production of H_2O_2 by primary hepatocytes and hepatic stellate cells (HSCs). (A–B). Primary hepatocytes (A) and HSC LX-2 cells (B) were treated for 30 min with 400 μM palmitate (n = 3). Co-IP analysis of the interaction between $p22^{phox}$, SH3YL1, and Nox4 in palmitate-treated WT hepatocytes. The cells were lysed, immunoprecipitated with an anti-SH3YL1 antibody, and the precipitates were immunoblotted with anti-Nox4 and anti-$p22^{phox}$ antibodies. A representative image is shown. (B–C). The H_2O_2 levels in palmitate-treated primary hepatocytes (C) and HSCs (D) from WT, SH3YL1$^{-/-}$, or Nox4$^{-/-}$ mice were detected by confocal microscopy of Peroxy Orange-1 fluorescence. (E–F). Primary hepatocytes from SH3YL1$^{-/-}$ mice were transfected with SH3YL1-Flag plasmid. (E) The hepatocytes were treated with palmitate and their H_2O_2 levels were detected by confocal microscopy of Peroxy Orange-1 fluorescence. (F) Their SH3YL1-Flag expression was analyzed by immunoblot analysis with antibody against Flag. In all plots, the data are shown as mean ± SEM. ns = not significant, *p < 0.05, **p < 0.01, ***p < 0.001, as determined by one-way ANOVA.

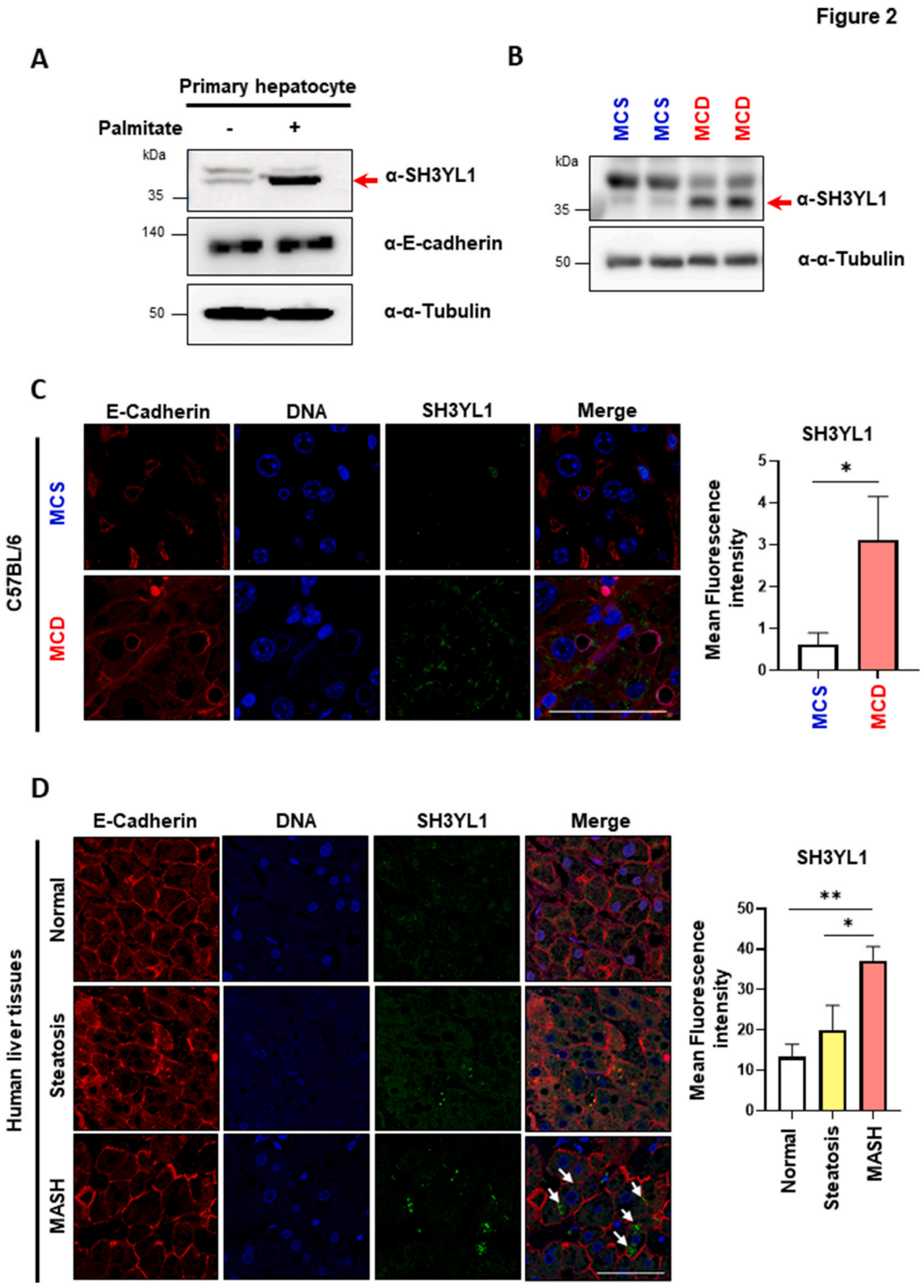

Fig. 2. SH3YL1 expression is upregulated in palmitate-treated primary hepatocytes, the liver of MCD diet-fed WT mice, and liver biopsies from MASH patients. (A) Primary WT hepatocytes were stimulated for 2 days with 400 μM palmitate. The cell lysates were subjected to immunoblot with antibodies against SH3YL1, E-cadherin, and α-tubulin. (B) Liver tissues were obtained from MCD diet fed C57BL/6 mouse. Tissue lysates were subjected to immunoblot with antibodies against SH3YL1 and α-tubulin. (C) Liver tissues were obtained from MCD diet fed C57BL/6 mouse. Each sample were stained with antibodies against SH3YL1 (green) and E-cadherin (red). Expression was monitored by confocal microscopy. Magnification of confocal microscopy is 400-fold. (n = 5, scale bar = 50 μm) Data are shown by means ± SEM; *$p < 0.05$, as determined by *t*-test. (D) Liver biopsies from human patients with MASH (n = 8), steatosis (n = 5), or histologically confirmed healthy liver (n = 7) were sectioned and stained with anti-SH3YL1 (green) or anti-E-cadherin (red) antibodies. (Left) Representative images (400-fold magnification; scale bar = 50 μm). The arrows indicate upregulated SH3YL1. (Right) Quantitation of SH3YL1 expression. The plot data are expressed as mean ± SEM. *$p < 0.05$, **$p < 0.01$, as determined by *t*-test (C) or one-way ANOVA (D).

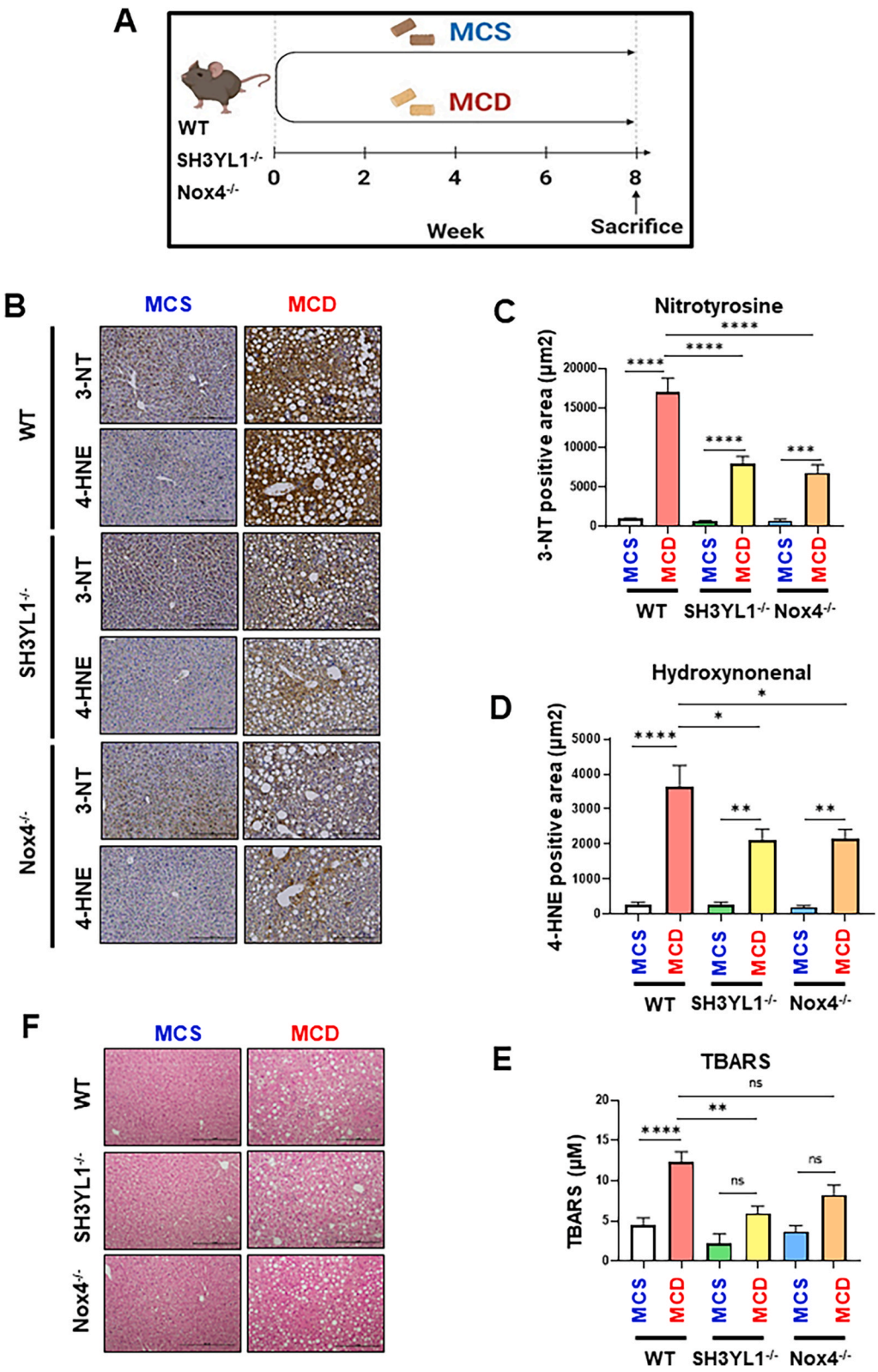

Fig. 3. MCD diet-fed SH3YL1$^{-/-}$ and Nox4$^{-/-}$ mice demonstrate reduced liver oxidative stress but not steatosis. (A) Schematic depiction of the generation of MASH with the MCD diet. Eight-week-old mice were fed the MCD or control MCS diet for 8 weeks. (B–F) WT, SH3YL1$^{-/-}$, and Nox4$^{-/-}$ mice were fed a MCD or MCS diet. (B) Immunohistochemistry of 3-NT and 4-HNE in the liver (n = 9–10). Representative images are shown (scale bar = 200 μm). (C) Quantification of 3-NT (n = 9–10). (D) Quantification of 4-HNE (n = 9–10). (E) Assessment of hepatic malonaldehyde levels by using a TBARS kit (n = 9–10). (F) Representative images of H&E-stained liver tissues (n = 14–16) (scale bar = 200 μm). In all plots, the data are shown as mean ± SEM. In C-E, *p < 0.05, **p < 0.01, ***p < 0.001, ****p < 0.0001, as determined by one-way ANOVA.

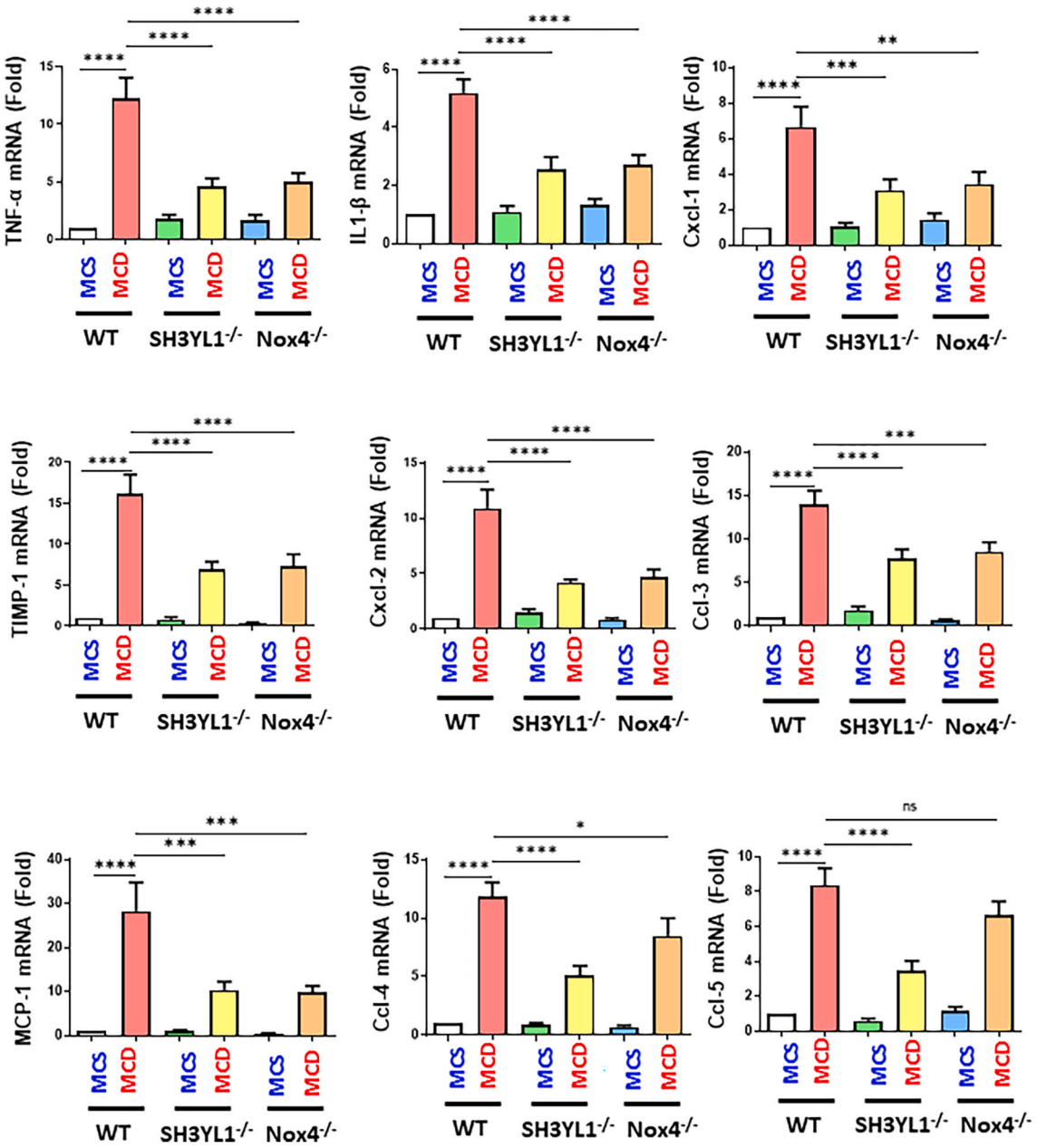

Fig. 4. The mRNA levels of inflammatory chemokines and cytokines from liver tissue of SH3YL1−/− and Nox4 mice fed MCD diet were measured by quantitative RT-PCR. The mRNA level of TNF- α, IL-1β, Cxcl-1, TIMP-1, Cxcl-2, Ccl-3, Ccl-4, Ccl-5, and MCP-1 in MCD fed SH3YL1$^{-/-}$ and Nox4$^{-/-}$ mice (n = 18~20). Data are expressed as fold over control values from MCD-fed WT mice. Data are shown as means ± SEM; *p < 0.05, **p < 0.01, ***p < 0.001, ****p < 0.0001, ns, not significant, as determined by one-way ANOVA.

3.5. Mice specifically lacking SH3YL1 expression in hepatocytes display less MCD diet-induced ROS, inflammation, injury, and fibrosis in the liver

To validate the role of hepatic SH3YL1 in MASH pathogenesis, we generated Alb-Cre/SH3YL1$^{fl/fl}$ mice in which hepatocyte-specific SH3YL1 is conditionally knocked out (Fig. S8A). The hepatocyte-specific knockout of SH3YL1 was proven by western-blot analysis of the primary hepatocytes from control Alb-Cre and Alb-Cre/SH3YL1$^{fl/fl}$ mice (Fig. S8B). Additionally, the expression levels of Nox1 and Nox4 in hepatocyte of Alb-Cre/SH3YL1$^{fl/fl}$ mice were similar with those in WT (Fig. S9). While Nox2 showed a slight decrease, p22phox increased slightly, suggesting that this may compensate for the decrease in Nox2. Overall, it appears that the expression of various Nox isozymes in SH3YL1 KO mice are similar with those in WT. MASH was then generated in the Alb-Cre/SH3YL1$^{fl/fl}$ mice with the MCD diet (Fig. 7A). Compared to the Alb-Cre mice, the Alb-Cre/SH3YL1$^{fl/fl}$ mice demonstrated significantly less oxidative stress in the liver, as shown by 3-NT and 4-HNE adduct levels (Fig. 7B–D). This confirmed that SH3YL1 in hepatocytes is specifically involved in the oxidative stress in MASH. However, this hepatocyte-specific SH3YL1 deficiency did not reduce steatosis, as indicated by the number and size of lipid droplets, as well as triglyceride levels and oil red O staining in the liver tissues (Fig. 7E, F, and S10).

We also found that hepatocyte-specific SH3YL1 deficiency reduced MCD diet-induced hepatic inflammation, as shown by less F4/80 staining (Fig. 8A and B). Hepatocyte-specific SH3YL1 deficiency also decreased MCD diet-induced hepatic injury, as indicated by lower TUNEL staining in liver (Fig. 8C and D). Moreover, the primary hepatocytes from Alb-Cre/SH3YL1$^{fl/fl}$ mice with palmitate resulted in suppressed cell death, compared to primary hepatocytes from control Alb-

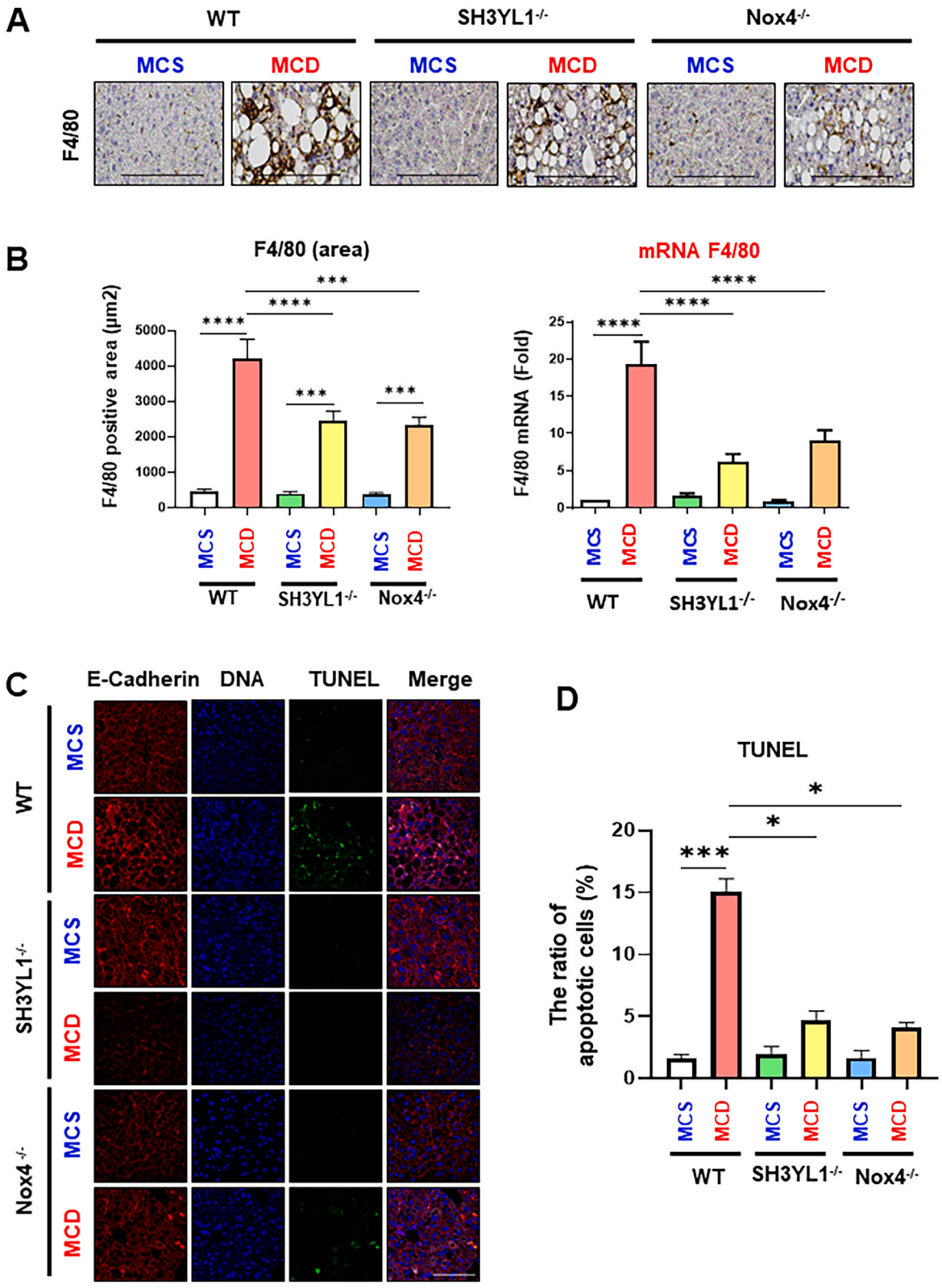

Fig. 5. MCD diet-fed SH3YL1$^{-/-}$ and Nox4$^{-/-}$ mice exhibit decreased liver inflammation and hepatocyte apoptosis. WT, SH3YL1$^{-/-}$, and Nox4$^{-/-}$ mice were fed the MCD or control MCS diet. (A–B) Immunohistochemistry (IHC) of F4/80 expression in the liver tissues from MCS- or MCD-fed WT, SH3YL1$^{-/-}$ and Nox4$^{-/-}$ mice (n = 9–10). (A) Representative images (scale bar = 200 μm). Quantification of F4/80 (left panel of B) from IHC (A) and the mRNA level of F4/80 (right panel of B) in MCS- or MCD-fed WT SH3YL1$^{-/-}$ and Nox4$^{-/-}$ mice (n = 18~20). (C–D) TUNEL-positive apoptotic hepatocytes in the liver (n = 4–6). (C) Representative images (scale bar = 100 μm). (D) Quantification of TUNEL-positive hepatocytes. In all plots, the data are shown as mean ± SEM. In B, C, **p < 0.01, ***p < 0.001, ****p < 0.0001, as determined by one-way ANOVA. In E, *p < 0.05, ***p < 0.001, as determined by mixed-effect analysis.

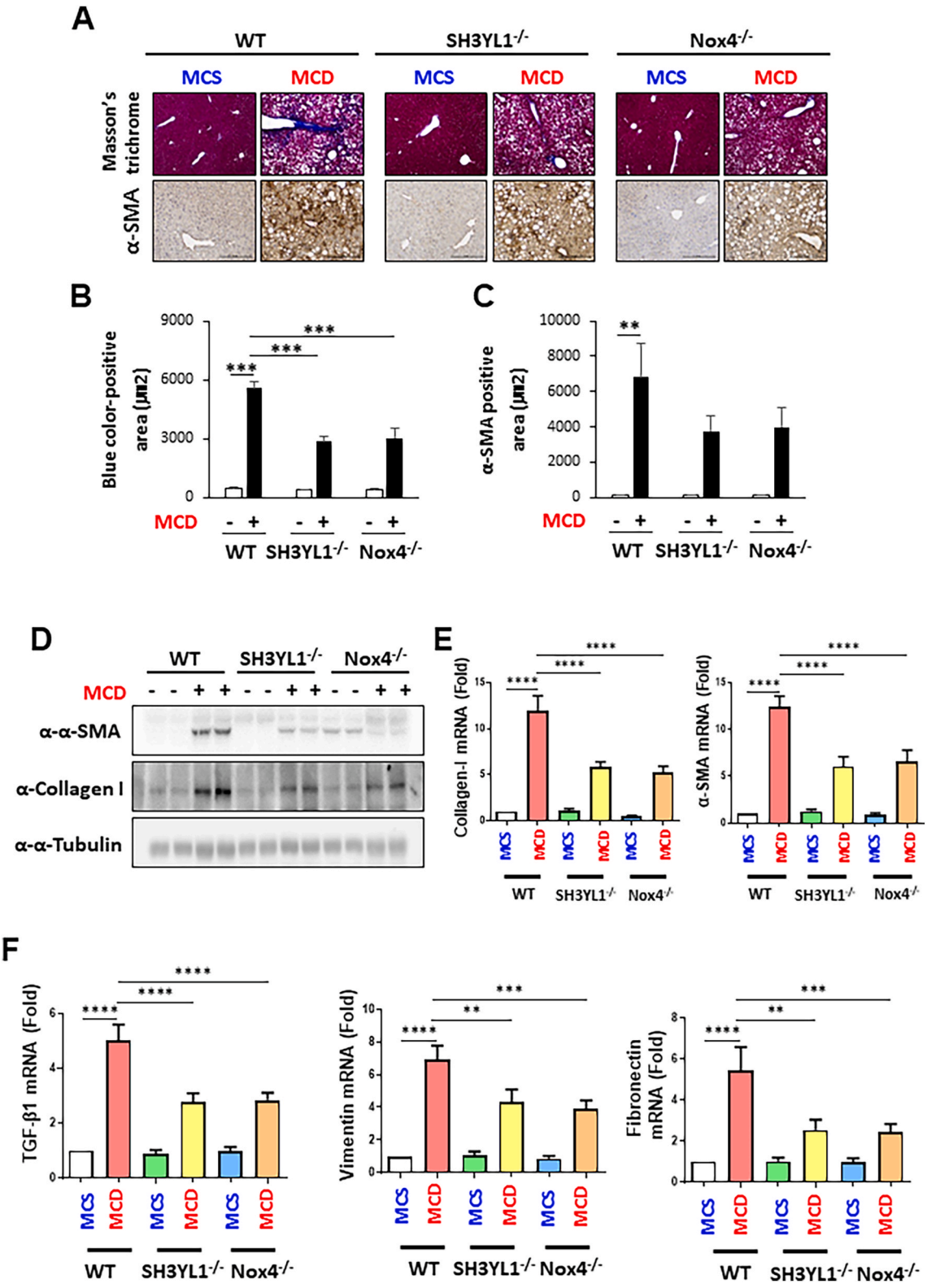

Fig. 6. MCD diet-fed SH3YL1$^{-/-}$ and Nox4$^{-/-}$ mice display less fibrosis. WT, SH3YL1$^{-/-}$, and Nox4$^{-/-}$ mice were fed the MCD or control MCS diet. (A–C). Immunohistochemistry of the liver with Masson's trichrome staining and α-SMA (n = 9–10). (A) Representative images (scale bar = 200 μm). (B) Quantification of Masson's trichrome staining. (C) Quantification of immunohistochemistry of α-SMA expression. (D) Representative immunoblot analysis of collagen-I and α-SMA protein expression (n = 3). (E, F) The mRNA levels from liver tissues of SH3YL1$^{-/-}$ and Nox4$^{-/-}$ mice fed MCD diet were measured by quantitative RT-PCR. The mRNA levels of Collagen-I (left panel of E), α-SMA (right panel of E), TGF-β1 (left panel of F), vimentin (middle panel of F), and fibronectin (right panel of F) (n = 18~20). Data are expressed as fold over control values from MCS-fed WT mice. Data are shown as means ± SEM; **p < 0.01, ***p < 0.001, ****p < 0.0001, as determined by one-way ANOVA.

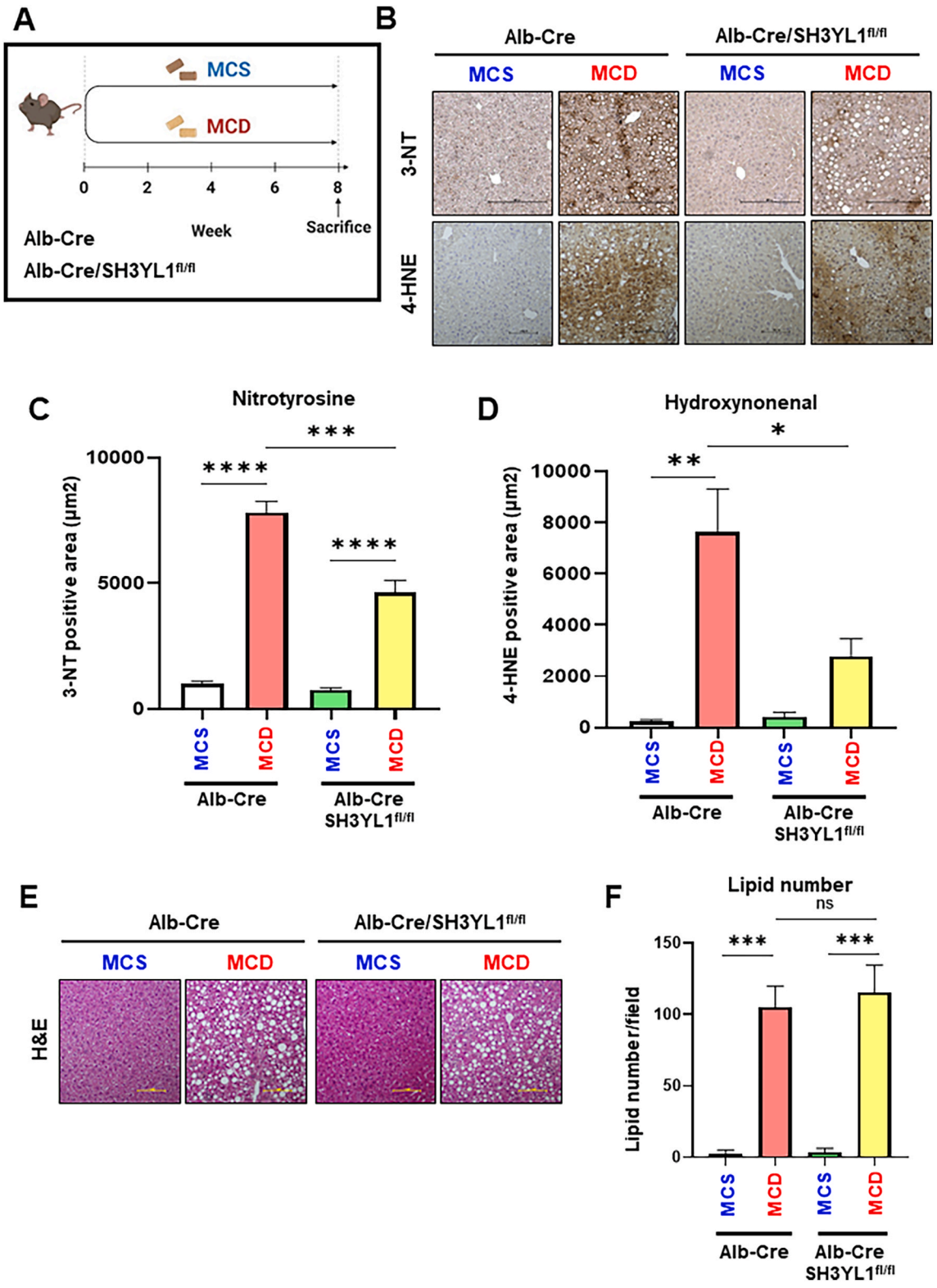

Fig. 7. MCD diet-fed Alb-Cre/SH3YL1$^{fl/fl}$ mice demonstrate reduced oxidative stress in the liver but similar steatosis. (A) Schematic depiction of MCD diet-induced MASH in Alb-Cre/SH3YL1$^{fl/fl}$ and control Alb-Cre mice. (B–D) Immunohistochemistry of 3-NT and 4-HNE in the liver (n = 10–11). (B) Representative images of 3-NT levels (scale bar = 200 μm) and 4-HNE levels (scale bar = 100 μm). (C) Quantification of 3-NT. (D) Quantification of 4-HNE. (E, F) H&E staining of the liver (n = 11–12). (E) Representative images (scale bar = 100 μm). (F) Quantification of H&E staining. All plot data are shown as mean ± SEM. ns = not significant, *p < 0.05, **p < 0.01, ***p < 0.001, as determined by mixed-effect analysis.

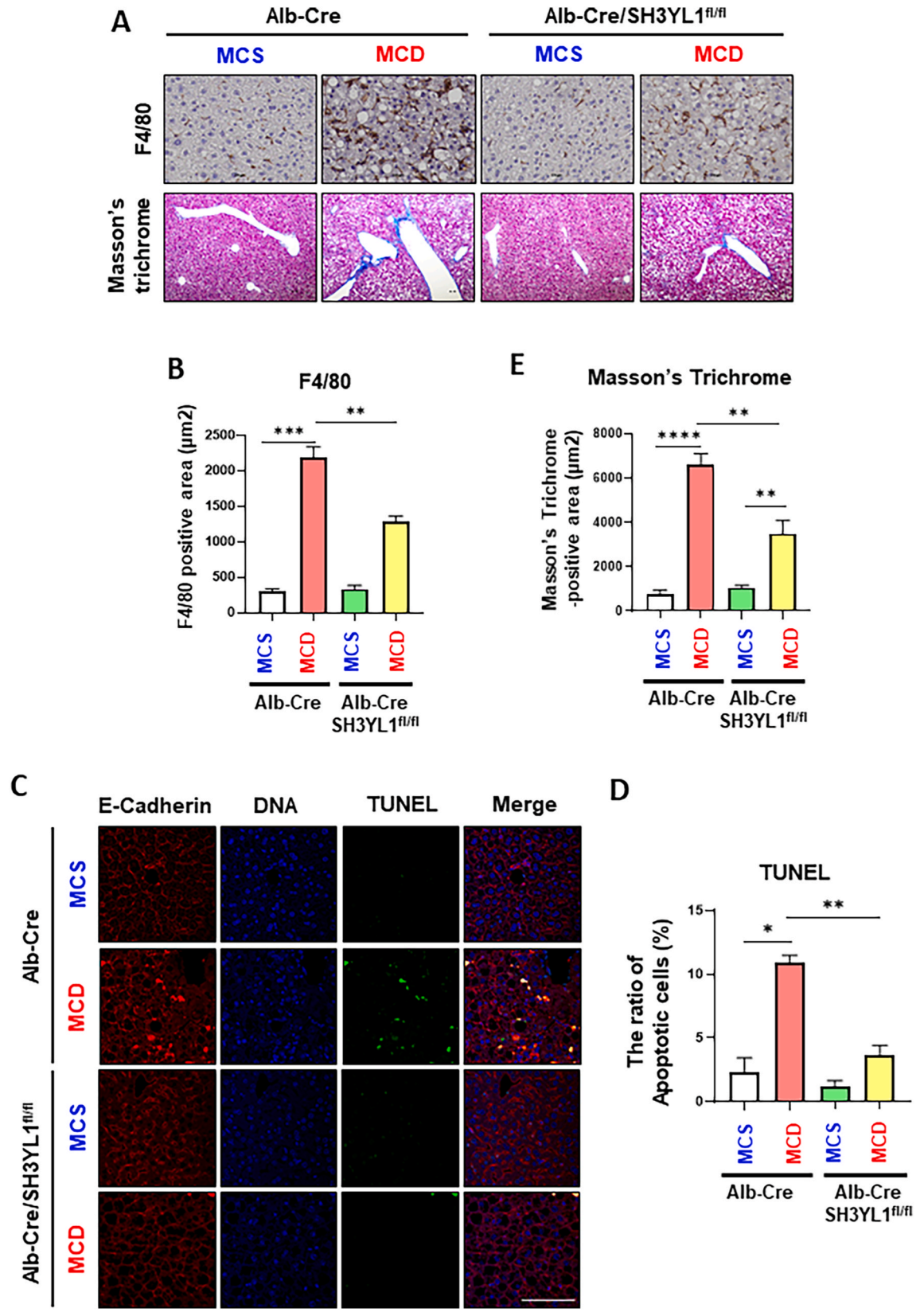

Fig. 8. MCD diet-fed Alb-Cre/SH3YL1$^{fl/fl}$ mice display less inflammation, fibrosis, and hepatocyte apoptosis. Alb-Cre/SH3YL1$^{fl/fl}$ and control Alb-Cre mice were fed the MCD or control MCS diet. (A–B) Immunohistochemistry of F4/80 (n = 8–10) and Collagen-I (Masson's trichrome stain) (n = 10–11) levels in the liver tissues from Alb-Cre/SH3YL1$^{fl/fl}$ and control Alb-Cre mice. (A) Representative images of F4/80 expression (scale bar = 200 μm) and Masson's trichrome staining (scale bar = 200 μm). (B) Quantification of F4/80 from (A). (C, D) TUNEL-positive cells in the liver (n = 4–5). (C) Representative images (scale bar = 100 μm). (D) Number of TUNEL-positive cells. (E) Quantification of Masson's trichrome staining from (A). All plot data are shown as mean ± SEM. ns = not significant, *p < 0.05, **p < 0.01, ***p < 0.001, ****p < 0.0001, as determined by mixed-effect analysis.

cre mice (Fig. S11). In addition, hepatocyte-specific SH3YL1 deficiency reduced MCD diet-induced liver fibrosis, as shown by Masson's trichrome (Fig. 8A and E) and Sirius red staining (Fig. S12). Thus, SH3YL1 plays an essential role in oxidative stress, inflammation, injury, and fibrosis in the liver in a murine MASH model.

4. Discussion

MAFLD encompasses a spectrum of liver disease, ranging from simple non-inflammatory steatosis such as MAFL to a more aggressive and advanced form of the disease called MASH [36–38]. Various risk factors including oxidative stress, hepatocellular injury, and fibrosis are associated with the progression of MASH. Interestingly, several lines of evidence have indicated that the level of ROS, an index of cellular oxidative stress, plays an important role in the pathogenesis of MASH [17–20]. There are various ROS sources including the mitochondrial respiratory chain, cyclooxygenase, the metabolism of fatty acids, and activation of Nox isozymes in liver tissues. Among them, Nox isozymes play important roles in MASH. Although Nox4 is a major isozyme in hepatocytes and is known to be involved in MASH, the regulation mechanism for Nox4 in MASH development is far from clear. However, we also found recently that Nox4 is also activated by other mechanisms, namely, the novel cytosolic regulator SH3YL1: we showed with renal tubular-epithelial cells that (i) SH3YL1 binds constitutively to Nox4, (ii) LPS or TGFβ1 treatment induces SH3YL1 tyrosine phosphorylation, (iii) this phosphorylation event causes the PRR of $p22^{phox}$ to bind to the SH3 domain of SH3YL1, and (iv) the binding of $p22^{phox}$ to the SH3YL1-Nox4 complex activates Nox4 enzymatic activity, thereby generating H_2O_2 [23,24].

The present study extends these findings from the chronically diseased kidney to the liver in MASH: we showed that SH3YL1 also bound constitutively to Nox4 in hepatocytes and HSCs, that the saturated fatty acid palmitate induced the SH3YL1-Nox4 complex to interact with p22phox, and that this increased H_2O_2 production by the hepatocytes and HSCs in vitro (Fig. 1). Our experiments with MCD diet-fed whole-body $SH3YL1^{-/-}$, $Nox4^{-/-}$, and hepatocyte-specific SH3YL1 conditional knockout mice then showed that the excessive H_2O_2 produced by the hepatocytes oxidatively modified lipids and proteins in the liver, as indicated by upregulated levels of 3-NT, 4-HNE, and malonaldehyde (Figs. 3 and 7). Thus, the Nox4-SH3YL1 complex in hepatocytes and HSCs promotes the oxidative stress in MASH (Fig. 9). Interestingly, Nox4-SH3YL1 axis did not contribute to the formation of

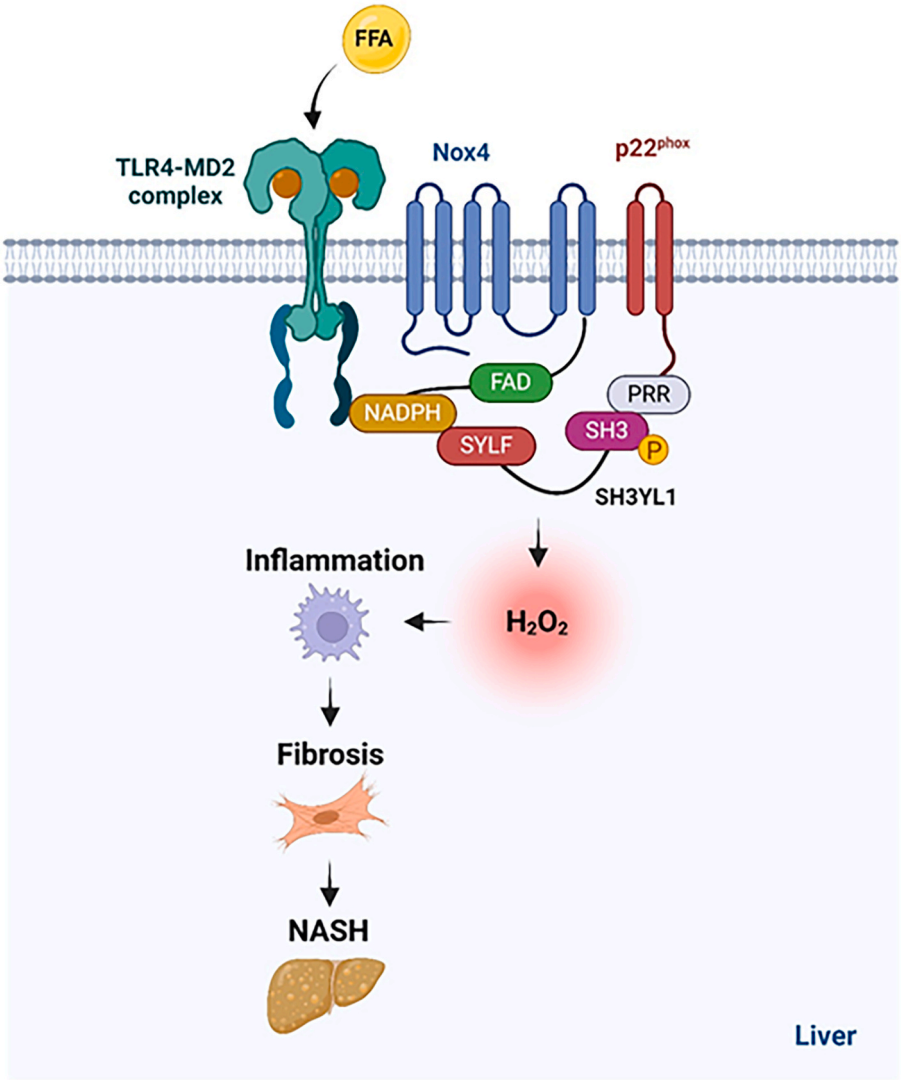

Fig. 9. Model for Nox4-SH3YL1-mediated H_2O_2 generation in MASH. Nox4 and SH3YL1 interact constitutively in hepatocytes. Increased free fatty acids (FFA) induce tyrosine phosphorylation in SH3YL1, which causes the PPR region of $p22^{phox}$ to interact with the SH3 region in SH3YL1, thereby generating a ternary Nox4-SH3YL1-$p22^{phox}$ complex. This causes the Nox4 in the hepatocytes to produce H_2O_2, which promotes oxidative stress, inflammation, hepatocyte death, and fibrosis in the liver and therefore the emergence of MASH.

lipid droplet in MCD diet-fed whole body SH3YL1$^{-/-}$, Nox4$^{-/-}$, and hepatocyte-specific SH3YL1 conditional knockout mice. However, further research is needed to understand the effects of Nox4-SH3YL1 pathway on lipid production in MCD diet-induced MASH model.

MCD-dependent fat accumulation in liver tissues is critical event in the pathogenesis of MASH [29]. Whole body knockout of SH3YL1 partly suppressed fat accumulation in liver tissues in response to MCD diet (Fig. 3F, S4 and S5). However, hepatocyte-specific conditional knockout SH3YL1 failed to stimulate fat accumulation in liver tissues in response to MCD diet (Fig. 7E and F, and S10). The steatosis observed in the whole-body knockout of SH3YL1 in response to the MCD diet suggests that the function of SH3YL1 in tissues other than hepatocytes may have partially contributed to fat accumulation. Specifically, it appears that the generation of hepatic microenvironments by SH3YL1 present in hepatic stellate cells (HSCs), Kupffer cells, and endothelial cells may contribute to the increased steatosis. How SH3YL1 in hepatic cells communicates with various cell signaling networks, such as MAPK and NF-κB in HSCs, Kupffer cells, and endothelial cells to regulate steatosis during the pathogenic processes of MASH remains to be elucidated.

Liver inflammation associates closely with the development of MASH [39,40]. Several lines of evidence indicate that Nox4 is activated indirectly by exogenous (LPS from gram-negative bacteria) and endogenous (saturated fatty acid such as palmitate) ligands, which bind to myeloid-differentiation factor 2 (MD2) on the cell surface. Since MD2 is an accessory protein of Toll-like receptor 4 (TLR4), this binding event activates TLR4. This in turn stimulates NF-kB and its downstream inflammatory responses, which then drive MASH [39–41]. Our study shows that Nox4-SH3YL1 axis in hepatocytes also regulates the liver inflammation in MASH (Figs. 4, 5 and 8). Specifically, mice lacking whole-body Nox4 or SH3YL1, or hepatocyte-specific SH3YL1, demonstrated suppressed pro-inflammatory cytokine expression and macrophage infiltration in the liver when they were fed a MCD diet. Notably, the SH3YL1-Nox4 axis may induce liver inflammation by being a component of the palmitate TLR4-Nox4 axis since (i) we previously found that LPS-induced binding of Nox4 to TLR4 causes endothelial cells to activate NF-kB and produce pro-inflammatory cytokines [42], (ii) free fatty acids induce inflammatory responses through TLR4 (Fig. 9) [40].

However, it should be noted that TLR4 can also act indirectly to induce liver ROS and inflammation in MASH by targeting the Nox2 isozyme; our studies on atherosclerosis showed that minimmaly-oxidized low density lipoprotein activates TLR4 in macrophages, which then sequentially activates spleen-tyrosine kinase, phospholipase Cγ1, protein kinase C, and finally Nox2. This sequence stimulates the macrophages to produce pro-inflammatory cytokines [43]. Since TLR4 is expressed not only by hepatocytes but also Kupffer cells and neutrophils, all of which have been implicated in MASH, it is possible that a more indirect palmitate-TLR4-Nox2 axis in these cells as well as in hepatocytes may also contribute to live inflammation in MASH. Indeed, Nox2 has been shown to promote pro-inflamamtory phenotypes in Kupffer cells in MAFLD. Another point of interest is that SH3YL1 does not activate Nox1 or Nox2 [23], which indicates that the ROS and inflammation induced by the SH3YL1-Nox4 axis in our MASH model mice is specific to Nox4 (Fig. 9). Moreover, while Nox4 is the main Nox isozyme in hepatocyte and HSCs and endothelial cells also express Nox4. Thus, the SH3YL1-Nox4 axis may also shape ROS production and pro-inflammatory activity in other liver cells types. Further research is needed to determine how Nox1, Nox2, and Nox4 in each live cells type contribute to MASH.

Both oxidative stress and inflammation cause hepatocyte death in MASH, as shown by increased TUNEL-positive hepatocyte numbers in MASH patients [44]. We also found that MCD diet-fed WT mice exhibited hepatocyte apoptosis. This was mediated by the SH3YL1-Nox4 axis since SH3YL1$^{-/-}$, Nox4$^{-/-}$, and hepatocyte-specific SH3YL1 conditional knockout mice exhibited much less MCD diet-induced liver injury (Figs. 5 and 8). The liver injury in MASH promotes fibrosis because it is an outcome of the wound-healing process. Hepatic fibrosis is characterized by the accumulation of extracellular matrix (ECM). When hepatocytes are injured by oxidative stress and inflammation, they both secrete fibrogenic cytokines and express ECM [45]. Indeed, we found that MCD diet-fed WT mice demonstrated enhanced Collagen-I expression in the liver. This too was mediated by the SH3YL1-Nox4 axis since this response to the MCD diet was much reduced in SH3YL1$^{-/-}$, Nox4$^{-/-}$, and hepatocyte-specific SH3YL1-knockout mice (Figs. 6 and 8).

Finally, we noted that hepatocytes from not only MCD diet-fed WT mice but also MASH patients demonstrated upregulation of SH3YL1 expression (Fig. 2). This upregulation was much less evident in hepatocytes from steatosis patients, and largely absent in patients with histologically normal livers. These findings together with our experiments showing that the Nox4-SH3YL1 axis drives hepatic ROS, inflammation, hepatocyte apoptosis, and fibrosis in MASH model mice suggests that this axis may also participate in MASH in humans (Fig. 9). However, this possibility must be tested with further studies. Several lines of evidence indicate that the Nox1, Nox2, and Nox4 isozymes, which are expressed in various cells such as hepatocytes, HSCs, and Kupffer cells within liver tissues, are involved in liver fibrosis and MASH [21,46]. Based on previous reports, the Nox1/4 inhibitor GKT137831 has demonstrated pharmacological efficacy in various MASH models [47–49]. Interestingly, Nox4 expression was significantly upregulated in liver biopsies from patients with stage 2/3 autoimmune hepatitis [50] and with NASH [21]. In patients with Nox4 overexpression, targeting the SH3YL1-Nox4 complex is expected to enhance pharmacological efficacy and reduce side effects. The development of such drug targets will be beneficial for creating more effective treatments for liver fibrosis.

5. Conclusion

We found that SH3YL1 serves as a Nox4 regulator in hepatic inflammation and fibrosis during MASH development. The mechanism may involve free fatty acid-dependent activation of the Nox4-SH3YL1 complex in hepatocytes. The activated Nox4-SH3YL1 complex in the hepatocytes then generates abundant H_2O_2, which leads to protein and lipid oxidation in the liver that in turn drives hepatic inflammation and injury. Ultimately, this results in the accumulation of ECM and hepatic fibrosis. Thus, the SH3YL1-Nox4 complex may play an important role in MASH pathogenesis.

CRediT authorship contribution statement

Yeo Kyu Hur: Methodology, Investigation, Formal analysis, Data curation, Conceptualization. **Hye Eun Lee:** Methodology, Investigation, Formal analysis, Data curation, Conceptualization. **Jung-Yeon Yoo:** Methodology, Investigation, Formal analysis, Data curation. **Young Nyun Park:** Resources, Methodology, Investigation. **In Hye Lee:** Writing – original draft, Supervision, Investigation, Funding acquisition. **Yun Soo Bae:** Writing – original draft, Supervision, Investigation, Funding acquisition.

Data availability statement

The datasets used and/or analyzed during the current study are available from the corresponding author on reasonable request.

Declaration of competing interest

The authors state no conflict of interest.

Acknowledgments

Fund was provided by the National Research Foundation of Korea (NRF) grant funded by the Korea government (MSIT) [RS-2024-00398295 to Y.S.B and NRF-2021R1A2C1091259 to I.H.L.] and by the

Starting growth Technological R&D Program (20165925) funded by the Ministry of SMEs and Startups (MSS, Korea).

Appendix A. Supplementary data

Supplementary data to this article can be found online at https://doi.org/10.1016/j.freeradbiomed.2024.12.021.

References

[1] Z.M. Younossi, P. Golabi, J.M. Paik, A. Henry, C. Van Dongen, L. Henry, The global epidemiology of nonalcoholic fatty liver disease (NAFLD) and nonalcoholic steatohepatitis (NASH): a systematic review, Hepatology 77 (4) (2023) 1335–1347.

[2] G. Parthasarathy, X. Revelo, H. Malhi, Pathogenesis of nonalcoholic steatohepatitis: an overview, Hepatol. Commun. 4 (4) (2020) 478–492.

[3] J.K. Dowman, J.W. Tomlinson, P.N. Newsome, Pathogenesis of non-alcoholic fatty liver disease, QJM: Int. J. Med. 103 (2) (2010) 71–83.

[4] X. Xu, K.L. Poulsen, L. Wu, S. Liu, T. Miyata, Q. Song, Q. Wei, C. Zhao, C. Lin, J. Yang, Targeted therapeutics and novel signaling pathways in non-alcohol-associated fatty liver/steatohepatitis (NAFL/NASH), Signal Transduct. Targeted Ther. 7 (1) (2022) 287.

[5] W.R. Kim, R.S. Brown Jr., N.A. Terrault, H. El-Serag, Burden of liver disease in the United States: summary of a workshop, Hepatology 36 (1) (2002) 227–242.

[6] L.S. Szczepaniak, P. Nurenberg, D. Leonard, J.D. Browning, J.S. Reingold, S. Grundy, H.H. Hobbs, R.L. Dobbins, Magnetic resonance spectroscopy to measure hepatic triglyceride content: prevalence of hepatic steatosis in the general population, Am. J. Physiol. Endocrinol. Metab. 288 (2) (2005) E462–E468.

[7] P. Sangwung, K.F. Petersen, G.I. Shulman, J.W. Knowles, Mitochondrial dysfunction, insulin resistance, and potential genetic implications, Endocrinology 161 (4) (2020).

[8] K. Cusi, Role of insulin resistance and lipotoxicity in non-alcoholic steatohepatitis, Clin. Liver Dis. 13 (4) (2009) 545–563.

[9] I.A. Kirpich, L.S. Marsano, C.J. McClain, Gut–liver axis, nutrition, and non-alcoholic fatty liver disease, Clin. Biochem. 48 (13) (2015) 923–930.

[10] E. Buzzetti, M. Pinzani, E.A. Tsochatzis, The multiple-hit pathogenesis of non-alcoholic fatty liver disease (NAFLD), Metabolism 65 (8) (2016) 1038–1048.

[11] A.P. Delli Bovi, F. Marciano, C. Mandato, M.A. Siano, M. Savoia, P. Vajro, Oxidative stress in non-alcoholic fatty liver disease. An updated mini review, Front. Med. 8 (2021) 595371.

[12] J.X. Jiang, N.J. Török, NADPH oxidases in chronic liver diseases, Adv Hepatol 2014 (2014).

[13] E. Crosas-Molist, I. Fabregat, Role of NADPH oxidases in the redox biology of liver fibrosis, Redox Biol. 6 (2015) 106–111.

[14] Y.S. Bae, H. Oh, S.G. Rhee, Y.D. Yoo, Regulation of reactive oxygen species generation in cell signaling, Mol. Cell 32 (6) (2011) 491–509.

[15] K. Bedard, K.H. Krause, The NOX family of ROS-generating NADPH oxidases: physiology and pathophysiology, Physiol. Rev. 87 (1) (2007) 245–313.

[16] H. Buvelot, V. Jaquet, K.H. Krause, Mammalian NADPH oxidases, Methods Mol. Biol. 1982 (2019) 17–36.

[17] T. Luangmonkong, S. Suriguga, H.A.M. Mutsaers, G.M.M. Groothuis, P. Olinga, M. Boersema, Targeting oxidative stress for the treatment of liver fibrosis, Rev. Physiol. Biochem. Pharmacol. 175 (2018) 71–102.

[18] Z. Chen, R. Tian, Z. She, J. Cai, H. Li, Role of oxidative stress in the pathogenesis of nonalcoholic fatty liver disease, Free Radic. Biol. Med. 152 (2020) 116–141.

[19] C. García-Ruiz, J.C. Fernández-Checa, Mitochondrial oxidative stress and antioxidants balance in fatty liver disease, Hepatol Commun. 2 (12) (2018) 1425–1439.

[20] Y.H. Paik, J. Kim, T. Aoyama, S. De Minicis, R. Bataller, D.A. Brenner, Role of NADPH oxidases in liver fibrosis, Antioxidants Redox Signal. 20 (17) (2014) 2854–2872.

[21] A. Bettaieb, J.X. Jiang, Y. Sasaki, T.I. Chao, Z. Kiss, X. Chen, J. Tian, M. Katsuyama, C. Yabe-Nishimura, Y. Xi, C. Szyndralewiez, K. Schröder, A. Shah, R.P. Brandes, F. G. Haj, N.J. Török, Hepatocyte nicotinamide adenine dinucleotide phosphate reduced oxidase 4 regulates stress signaling, fibrosis, and insulin sensitivity during development of steatohepatitis in mice, Gastroenterology 149 (2) (2015) 468, 80. e10.

[22] T. Lan, T. Kisseleva, D.A. Brenner, Deficiency of NOX1 or NOX4 prevents liver inflammation and fibrosis in mice through inhibition of hepatic stellate cell activation, PLoS One 10 (7) (2015) e0129743.

[23] J.Y. Yoo, D.R. Cha, B. Kim, E.J. An, S.R. Lee, J.J. Cha, Y.S. Kang, J.Y. Ghee, J. Y. Han, Y.S. Bae, LPS-induced acute kidney injury is mediated by nox4-sh3yl1, Cell Rep. 33 (3) (2020) 108245.

[24] S.R. Lee, H.E. Lee, J.Y. Yoo, E.J. An, S.J. Song, K.H. Han, D.R. Cha, Y.S. Bae, Nox4-SH3YL1 complex is involved in diabetic nephropathy, iScience 27 (2) (2024) 108868.

[25] H. Malhi, S.F. Bronk, N.W. Werneburg, G.J. Gores, Free fatty acids induce JNK-dependent hepatocyte lipoapoptosis, J. Biol. Chem. 281 (17) (2006) 12093–12101.

[26] K. Yamaguchi, L. Yang, S. McCall, J. Huang, X.X. Yu, S.K. Pandey, S. Bhanot, B. P. Monia, Y.X. Li, A.M. Diehl, Inhibiting triglyceride synthesis improves hepatic steatosis but exacerbates liver damage and fibrosis in obese mice with nonalcoholic steatohepatitis, Hepatology 45 (6) (2007) 1366–1374.

[27] H. Tilg, A.R. Moschen, Evolution of inflammation in nonalcoholic fatty liver disease: the multiple parallel hits hypothesis, Hepatology 52 (5) (2010) 1836–1846.

[28] D. Gabbia, L. Cannella, S. De Martin, The role of oxidative stress in NAFLD–NASH–HCC transition—focus on NADPH oxidases, Biomedicines 9 (6) (2021) 687.

[29] D.H. Ipsen, J. Lykkesfeldt, P. Tveden-Nyborg, Molecular mechanisms of hepatic lipid accumulation in non-alcoholic fatty liver disease, Cell. Mol. Life Sci. 75 (18) (2018) 3313–3327.

[30] T. Huby, E.L. Gautier, Immune cell-mediated features of non-alcoholic steatohepatitis, Nat. Rev. Immunol. 22 (7) (2022) 429–443.

[31] C. Luci, M. Bourinet, P.S. Leclère, R. Anty, P. Gual, Chronic inflammation in non-alcoholic steatohepatitis: molecular mechanisms and therapeutic strategies, Front. Endocrinol. 11 (2020).

[32] P. Dongiovanni, S. Stender, A. Pietrelli, R.M. Mancina, A. Cespiati, S. Petta, S. Pelusi, P. Pingitore, S. Badiali, M. Maggioni, V. Mannisto, S. Grimaudo, R. M. Pipitone, J. Pihlajamaki, A. Craxi, M. Taube, L.M.S. Carlsson, S. Fargion, S. Romeo, J. Kozlitina, L. Valenti, Causal relationship of hepatic fat with liver damage and insulin resistance in nonalcoholic fatty liver, J. Intern. Med. 283 (4) (2018) 356–370.

[33] R. Bataller, D.A. Brenner, Liver fibrosis, J. Clin. Invest. 115 (2) (2005) 209–218.

[34] S.L. Friedman, Liver fibrosis – from bench to bedside, J. Hepatol. 38 (Suppl 1) (2003) S38–S53.

[35] Y. Koyama, D.A. Brenner, Liver inflammation and fibrosis, J. Clin. Invest. 127 (1) (2017) 55–64.

[36] J.P. Arab, M. Arrese, M. Trauner, Recent insights into the pathogenesis of nonalcoholic fatty liver disease, Annu. Rev. Pathol. 13 (2018) 321–350.

[37] V.T. Samuel, G.I. Shulman, Nonalcoholic fatty liver disease as a nexus of metabolic and hepatic diseases, Cell Metabol. 27 (1) (2018) 22–41.

[38] A.C. Sheka, O. Adeyi, J. Thompson, B. Hameed, P.A. Crawford, S. Ikramuddin, Nonalcoholic steatohepatitis: a review, JAMA 323 (12) (2020) 1175–1183.

[39] S.Y. Kim, J.-M. Jeong, S.J. Kim, W. Seo, M.-H. Kim, W.-M. Choi, W. Yoo, J.-H. Lee, Y.-R. Shim, H.-S. Yi, Y.-S. Lee, H.S. Eun, B.S. Lee, K. Chun, S.-J. Kang, S.C. Kim, B. Gao, G. Kunos, H.M. Kim, W.-I. Jeong, Pro-inflammatory hepatic macrophages generate ROS through NADPH oxidase 2 via endocytosis of monomeric TLR4–MD2 complex, Nat. Commun. 8 (1) (2017) 2247.

[40] Y. Wang, Y. Qian, Q. Fang, P. Zhong, W. Li, L. Wang, W. Fu, Y. Zhang, Z. Xu, X. Li, G. Liang, Saturated palmitic acid induces myocardial inflammatory injuries through direct binding to TLR4 accessory protein MD2, Nat. Commun. 8 (2017) 13997.

[41] S. Das, F. Alhasson, D. Dattaroy, S. Pourhoseini, R.K. Seth, M. Nagarkatti, P. S. Nagarkatti, G.A. Michelotti, A.M. Diehl, B. Kalyanaraman, S. Chatterjee, NADPH oxidase–derived peroxynitrite drives inflammation in mice and human nonalcoholic steatohepatitis via TLR4-lipid raft recruitment, Am. J. Pathol. 185 (7) (2015) 1944–1957.

[42] H.S. Park, J.N. Chun, H.Y. Jung, C. Choi, Y.S. Bae, Role of NADPH oxidase 4 in lipopolysaccharide-induced proinflammatory responses by human aortic endothelial cells, Cardiovasc. Res. 72 (3) (2006) 447–455.

[43] Y.S. Bae, J.H. Lee, S.H. Choi, S. Kim, F. Almazan, J.L. Witztum, Y.I. Miller, Macrophages generate reactive oxygen species in response to minimally oxidized low-density lipoprotein, Circ. Res. 104 (2) (2009) 210–218.

[44] A.E. Feldstein, A. Canbay, P. Angulo, M. Taniai, L.J. Burgart, K.D. Lindor, G. J. Gores, Hepatocyte apoptosis and fas expression are prominent features of human nonalcoholic steatohepatitis, Gastroenterology 125 (2) (2003) 437–443.

[45] T. Tsuchida, S.L. Friedman, Mechanisms of hepatic stellate cell activation, Nat. Rev. Gastroenterol. Hepatol. 14 (7) (2017) 397–411.

[46] C.A. Piantadosi, H.B. Suliman, Redox regulation of mitochondrial biogenesis, Free Radic. Biol. Med. 53 (11) (2012) 2043–2053.

[47] T. Aoyama, Y.H. Paik, S. Watanabe, B. Laleu, F. Gaggini, L. Fioraso-Cartier, S. Molango, F. Heitz, C. Merlot, C. Szyndralewiez, P. Page, D.A. Brenner, Nicotinamide adenine dinucleotide phosphate oxidase in experimental liver fibrosis: GKT137831 as a novel potential therapeutic agent, Hepatology 56 (6) (2012) 2316–2327.

[48] D. Jones, M. Carbone, P. Invernizzi, N. Little, F. Nevens, M.G. Swain, P. Wiesel, C. Levy, Impact of setanaxib on quality of life outcomes in primary biliary cholangitis in a phase 2 randomized controlled trial, Hepatol. Commun. 7 (3) (2023) e0057.

[49] V.J. Thannickal, K. Jandeleit-Dahm, C. Szyndralewiez, N.J. Török, Pre-clinical evidence of a dual NADPH oxidase 1/4 inhibitor (setanaxib) in liver, kidney and lung fibrosis, J. Cell Mol. Med. 27 (4) (2023) 471–481.

[50] P. Mukhopadhyay, B. Horváth, Z. Zsengellér, S. Bátkai, Z. Cao, M. Kechrid, E. Holovac, K. Erdèlyi, G. Tanchian, L. Liaudet, I.E. Stillman, J. Joseph, B. Kalyanaraman, P. Pacher, Mitochondrial reactive oxygen species generation triggers inflammatory response and tissue injury associated with hepatic ischemia–reperfusion: therapeutic potential of mitochondrially targeted antioxidants, Free Radic. Biol. Med. 53 (5) (2012) 1123–1138.